Piezochromism in Nickel Salicylaldoximato Complexes: Tuning Crystal-Field Splitting with High Pressure

Manuscript received: 19/01/2012; Article published: 21/05/2012

Piezochromism in Nickel Salicylaldoximate Complexes: Tuning Crystal Field Splitting with High Pressure**

Peter J. Byrne,[1] Patricia J. Richardson,[1] John Chang,[1] Anna F. Kusmartseva,[1] David R. Allan,[2] Anita C. Jones,[1] Konstantin V. Kamenev,[3] Peter A. Tasker[1]* and Simon Parsons[1]*

[1]EaStCHEM, School of Chemistry, Joseph Black Building, University of Edinburgh, West Mains Road, Edinburgh, EH9 3JJ, UK.

[2]Diamond Light Source, Harwell Science and Innovation Campus, Didcot, Oxfordshire, UK.

[3]School of Engineering and Centre for Science at Extreme Conditions, Erskine Williamson Building, The University of Edinburgh, King's Buildings, West Mains Road, Edinburgh, Scotland EH9 3JJ, UK.

[*]Corresponding author; e-mail: s.parsons@ed.ac.uk, tel: +44-(0)131 650 4806, fax: +44-(0)131 650 4743

[**]We thank EPSRC for funding and Diamond Light Source for access to beamline I19 (proposal number MT1200) that contributed to the results presented here.

Supporting information:
Supporting information for this article is available on the WWW under http://dx.doi.org/10.1002/chem.201200213

Graphical abstract:

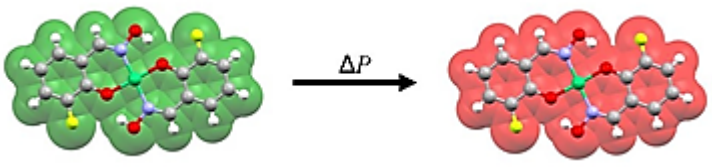

Synopsis:
High pressure reduces the Ni-O and Ni-N bond distances in nickel salicylaldoximate complexes tuning the crystal field experienced by the metal ion and leading to piezochromism.

Abstract

The crystal structures of bis(3-fluoro-salicylaldoximato)nickel(II) and bis(3-methoxy-salicylaldoximato)nickel(II) have been determined at room temperature between ambient pressure and approximately 6 GPa. The principal effect of pressure is to reduce intermolecular contact distances. In the fluoro-system molecules are stacked, and the Ni…Ni distance decreases from 3.19 Å at ambient pressure to 2.82 Å at 5.4 GPa. These data are similar to those observed in bis(dimethylglyoximato)nickel(II) over a similar pressure range, though by contrast with that system, and in spite of their structural similarity, the salicyloximate does not become conducting at high pressure. Ni-ligand distances also shorten, on average by 0.017 and 0.011 Å for the fluoro- and methoxy- complexes, respectively. Bond compression is small if the bond in question is directed towards an interstitial void. A band at 620 nm, which occurs in the visible spectrum of each derivative, can be assigned to a transition to an anti-bonding molecular orbital based on the metal 3d(x^2-y^2) orbital. Time-dependent density functional theory calculations show that the energy of this orbital is sensitive to pressure, increasing in energy as the Ni-ligand distances are compressed, and consequently increasing the energy of the transition. The resulting blue shift of the UV-visible band leads to piezochromism, and crystals of both complexes, which are green at ambient pressure, become red at 5 GPa.

1. Introduction

The idea that there is a close relationship between the structure of a material and its properties forms the basis of much modern research in materials and inorganic chemistry. Structure-property relationships are usually explored using numerous derivatives of a material, looking for specific structural features which correlate with a property of interest. One example of this was the development of the relationship between magnetic coupling and the bridging bond angle in bis(hydroxo)copper(II) dimers.[1] An alternative approach is to apply high pressure, monitoring structural distortions using single-crystal X-ray diffraction, and correlating these with physical property measurements also conducted at high pressure. The advantage of this approach, which is exemplified below, is that all measurements are made on the same material, and there is no need to make the assumption that changes in other parameters which occur on derivatisation are unimportant.

Over the past decade experimental techniques of high-pressure single-crystal diffraction have advanced substantially as the result of the introduction of area detectors and synchrotron sources. High-pressure structural work on organic compounds has aimed to produce new high-pressure phases by rearrangement of intermolecular interactions.[2] Although intramolecular conformational changes have also been observed in some of these studies, bond angles and distances are not greatly affected. For example, in serine hydrate some CC and CO bonds shortened by around 0.01 Å between ambient pressure and 3.8 GPa‡.[3] The same is not true

‡ The unit of pressure used here is the gigapascal (GPa). 1 atm = 1.01325×10^{-4} GPa. 1 GPa = 10 kbar ~ 10 000 atm. Pressures at the bottom of deep sea trenches reach around 1000 atm ~ 1 kbar = 0.1 GPa.

in coordination compounds, where metal geometry is more flexible. Changes in bond distances can be an order of magnitude greater than those seen in serine hydrate: in *cis*-$[PdCl_2([9]aneS_3]$, for example, a Pd…S distance changed by 0.31 Å between ambient pressure and 4.25 GPa.[4] In view of the importance of coordination complexes as functional materials, this feature makes transition metal complexes particularly attractive subjects for high-pressure studies exploring structure-property relationships.

The number of high-pressure crystal structure determinations of transition metal complexes has started to increase rapidly. A search of the Cambridge Structural Database (CSD)[5] for entries referring to transition metal compounds with the field *pressure* identified 135 crystal structure determinations at 0.1 GPa or above; of these almost half (66) were published in 2009-2010. Typically several data sets were collected for a compound as pressure was increased, and the number of individual compounds studied is therefore substantially less, around 35. Some studies have focussed on the compressibility of inter- and intra- molecular interactions; others are devoted to exploring structure-property relationships in magnetism, conductivity or porosity.

Intermolecular contacts generally prove to be substantially more compressible than intramolecular interactions. Compression of intermolecular interactions such as H-bonds and van der Waals contacts were explored in $[Ru_3(CO)_{12}]$ (CSD refcode FOKNEY)[6] to 8 GPa, $[Co_2(CO)_6(PPh_3)]$ (CEDBUJ)[7] to 4.6 GPa and $[4\text{-chloropyridinium}]_2[CoX_4]$ (X = Cl, Br) (SAZZID)[8] to 4 GPa. Intramolecular geometry may distort substantially in order to accommodate shorter contacts; in $[Co_2(CO)_6(PPh_3)]$, for example, the molecule adopts a nearly eclipsed conformation in order to avoid close carbonyl-phenyl contacts; similar features were observed in the arsenic analogue.[9] In $[4\text{-chloropyridinium}]_2[CoX_4]$ the $[CoX_4]^{2-}$ anion distorts in response to changes in the electric field which occur on compression.

In some cases intramolecular contacts have been converted into intramolecular bonds. The systems *cis*-$[PdCl_2([9]aneS_3]$ (CSD refcode GATLES)[4] and $[GuH][Cu_2(OH)(cit)(Gu)_2]$ (H_4cit = citric acid, Gu = guanidine and GuH = guanidinium cation),[10] have been shown to undergo phase transitions in which long intermolecular contacts involving the metal atoms have been transformed into primary coordination bonds; this occurred at 4.6 GPa, in the case of the Pd complex, and at 2.9 and 4.2 GPa for the Cu complex.

The ability to affect intramolecular interactions has prompted a number of groups to explore the ability of pressure to tune physical properties governed by metal-metal or metal-ligand distances or the geometry around bridging groups. In the field of magnetism this work has shown that pressure is a very powerful means for studying magneto-structural correlations. For example, in $[NMe_4][MnCl_3]$ (TMAMMN)[11] parallel structural and magnetic measurements revealed an approximate r^{-10} dependence of the coupling constant with Mn…Mn distance (r) pointing to the importance of direct exchange coupling between the metals.

Single-molecule magnets (SMMs) have also been studied in this context, and, apart from proteins, these are the most complex systems to have been investigated using high-pressure crystallography. Magnetic coupling

in SMMs is mediated via super-exchange and therefore depends on the geometry of bridging ligands. The torsional flexibility of bridging derivatised salicylaldoxime (R-saoH_2) ligands in [Mn_6O_2(Et-sao)$_6$(O_2CPh(Me)$_2$)$_2$(EtOH)$_6$] has enabled pressure to be used to reduce the magnitude of Mn-O-N-Mn torsion angles.[12] This changes the interaction between pairs of Mn atoms from ferromagnetic to antiferromagnetic, leading to a reduction in the spin ground state for the complex and a lowering of the energy barrier for the reorientation of its magnetic moment. In the Mn_{12}-carboxylate family of SMMs the existence of fast- and slow-relaxing species has been ascribed to the presence of Jahn-Teller isomers which differ in the orientation of the Jahn-Teller axis of a Mn(III) centre. A study on the complex [$Mn_{12}O_{12}$($O_2CCH_2{}^tBu$)$_{16}$(H_2O)$_4$]·CH_2Cl_2·$MeNO_2$ showed that these isomers can be inter-converted using pressure, with parallel magnetic measurements showing corresponding conversion between fast and slow relaxation of the magnetisation.[13]

High pressure has also been used to study spin-crossover complexes of Fe(II). Ambient pressure and temperature usually favour the high-spin state; this has a higher volume than the low-spin state owing to occupation of antibonding e_g orbitals, and so pressure favours the low-spin state because of the need to minimise the pV contribution to free energy. Pressure-induced high-to-low spin transitions have been observed by single crystal diffraction in [Fe(phen)$_2$(NCS)$_2$] (KEKVIF) and [Fe(Btz)$_2$(NCS)$_2$] (PASGOF), where phen = 1,10-phenanthroline and Btz = 2,2'-bi-4,5-dihydrothiazine, at 1 and 0.5 GPa, respectively.[14] Other transitions have been followed by changes in cell dimensions tracked using powder diffraction.[15]

The ability to compress intra- and inter-molecular interactions has also excited interest in the field of metal-organic framework materials, where pressure has the potential to control uptake of different guests. This has recently been described in a study in which the unit cell volume of the zeolitic imidazole framework ZIF-8 was shown to *increase* under pressure as solvent molecules were forced into the pores, leading eventually to a new phase with enlarged channels at 1.47 GPa.[16]

Piezochromism, the property of changing colour under pressure, has been studied using UV-visible absorption or luminescence as spectroscopic probes.[17] The origin of spectral changes with pressure may be due to modifications of intramolecular or intermolecular bonding. Intramolecular effects appear to be more common. For example, absorption bands in [Ni(H_2O)$_6$]SO_4 and [Ni(NH_3)$_6$]Cl_2 are blue-shifted at high pressure as the result of an increase in ligand field strength which occurs as ligand-metal distances shorten.[18]

Jahn-Teller distortions can be suppressed using pressure,[19] the direction of Jahn-Teller axes altered,[13, 20] and Jahn-Teller elongations converted into compressions.[21] The flexibility of the coordination geometry of copper has led to a number of studies of piezochromism in complexes of this metal. For example, [Cu(dieten)$_2$](BF_4)$_2$, containing the asymmetrically substituted N,N-diethylethylenediamine (dieten) ligand, contains four coordinate Cu at ambient pressure, with long Cu…F interactions to the anions. At 6 GPa UV-visible spectra suggest that a phase transition occurs which shortens the Cu…F distances leading to a colour change from red to orange-yellow.[22] A combined high-pressure UV-visible and crystallographic study of

[guanadinium]$_4$[Cu_2(citrate)$_2$].2H_2O demonstrated a similar effect, with a colour change from blue to green being associated with a decrease in a Cu…O(carboxylate) distance from 2.6238(3) to 2.407(3) Å.[23]

The use of pressure to control colour via intermolecular interactions has been studied extensively in four coordinate complexes of the group 10 metals. Glyoxime complexes have been studied particularly thoroughly, and these will be discussed in more detail in Section 4.2. Piezochromism in Pd complexes has been reviewed,[24] while that of one complex, bis(1,2-cyclo hexane dionedioximato) Pd(II), has led to its being suggested as a possible internal pressure marker.[25] Pt(bipy)Cl_2 converts from red to yellow at 1.75 GPa, as the result of a phase transition, though the crystal structure of the high-pressure form is unknown.[26] The closely related phenomenon of mechanochromism has been recently investigated in C_6F_5-Au-CN-C_6H_4-NC-Au-C_6F_5, for which a dramatic colour change from blue to yellow occurs on grinding as the result of shorter Au…Au interactions.[27]

Although transition metal complexes are attractive candidates for the study of pressure effects on electronic structures, studies where high-pressure spectroscopic data are combined with high-resolution, high-pressure single-crystal diffraction data are quite rare. The power of this approach is amply illustrated by the work on other the structure-property relationships described above, and there seems to be enormous scope for expanding research in this area. The subject of the present paper is an investigation of piezochromism in two nickel complexes of salicylaldoximes, bis(3-fluorosalicylaldoximato)nickel (**1**F) and bis(3-methoxysalicylaldoximato)nickel (**1**MeO) (see Scheme). We show that while nickel complexes of salicylaldoximes share many of the structural characteristics of glyoxime complexes, also exhibiting piezochromism, their spectral characteristics and the response of the spectra to high pressure are quite different.

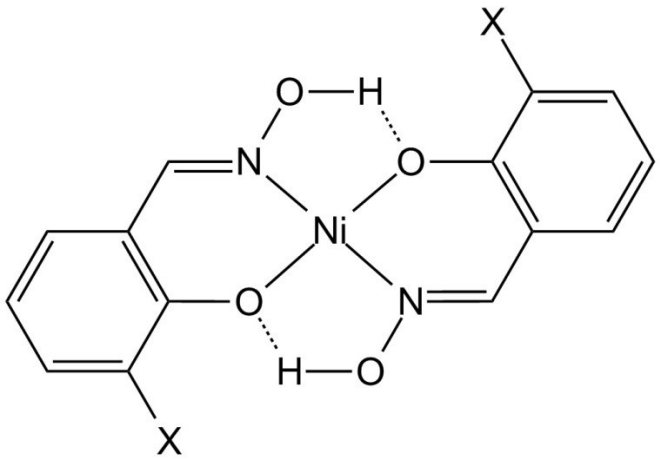

1F: X = F

1MeO: X = MeO

2. Experimental

*2.1 [Bis(3-fluorosalicylaldoximato)nickel(II)] (**1**F)*

$Ni(OAc)_2{\cdot}4H_2O$ (31 mg, 0.125 mmol) was added to 3-fluorosalicylaldoxime (32 mg, 0.206 mmol) in methanol (2 mL). A green precipitate formed immediately. The mixture was stirred overnight at room temperature, filtered, washed with methanol and then with ether to give a green solid which was dissolved in the minimum of hot THF and filtered. On cooling the filtrate gave crystalline **1**F (Yield = 51 mg, 67%). Elemental and crystallographic analysis are in agreement with the structural formula $NiC_{14}H_{10}F_2N_2O_4$ calculated C 45.83%, H 2.75%, N 7.63% found C 45.80%, H 2.62%, N 7.53%.

*2.2 [Bis(3-methoxysalicylaldoximato)nickel(II)] (**1**MeO)*

$Ni(OAc)_2{\cdot}4H_2O$ (20 mg, 0.080 mmol) was added to a yellow solution of 3-methoxysalicylaldoxime (20 mg, 0.120 mmol) in methanol (1 mL). The mixture was stirred overnight at room temperature, giving a green precipitate which was collected and washed with cold methanol. Recrystallisation was achieved by vapour diffusion of methanol into a THF solution (Yield = 25 mg, 53%). Elemental and crystallographic analysis are in agreement with the structural formula $NiC_{16}H_{16}N_2O_6$ calculated C 49.15%, H 4.12%, N 7.16%, found C 49.55%, H 3.74%, N 6.92%.

2.3 Crystallography

Diffraction data were collected on a single crystal of **1**F on an Agilent SuperNova diffractometer under ambient conditions of temperature and pressure. A multi-scan absorption correction was applied. The structure was solved by direct methods (SIR92)[28] and refined against F^2 using all data (CRYSTALS).[29] H-atoms were located in a difference map, and after idealising their positions, they were allowed to ride on their parent C or O atoms. All non-H atoms were modelled with anisotropic displacement parameters.

The structure of **1**MeO was first determined at ambient pressure by Li *et al.* at 173K;[30] the structure was re-determined at ambient temperature as part of this work so that all structures could be compared using data collected at the same temperature. Data collection and refinement procedures were the same as described above for **1**F.

For the high pressure experiments a single crystal of **1**F or **1**MeO was loaded into a Merrill-Bassett diamond anvil cell (half opening angle 40˚), equipped with Boehler-Almax-cut diamonds with 600 μm culets,[31] a tungsten gasket and tungsten carbide backing plates. A mixture of 4:1 methanol and ethanol was used as the pressure-transmitting medium. Pressure was measured using the ruby fluorescence method. Diffraction data were collected on a Rigaku Saturn 724+ CCD detector on Station I19 (λ = 0.5159 Å) at the Diamond Light

Source. The diffraction images were converted into Bruker format;[32] data processing procedures then followed ref. [33] Data were integrated to a resolution of 0.9 Å for **1**F, and to 0.8 Å for **1**MeO. Refinements were carried out against F^2 using all data (CRYSTALS) starting from the coordinates determined at ambient pressure. Refinement followed the same strategy as described above for the ambient-pressure determinations except that intramolecular distances and angles within the ligand were restrained to their ambient-pressure values. Distances and angles involving the metal atom were not restrained. Rigid body and rigid bond similarity restraints were also applied to the anisotropic displacement parameters of the light atoms.

Data were collected for **1**F to a maximum pressure of 6.1 GPa. Diffraction spots at this pressure were broad and split, while the *R*-factors obtained after refinement were almost three times those obtained at lower pressure. Therefore only data up to 5.4 GPa were used for further analysis. The maximum pressure obtained for the **1**MeO series was 5.6 GPa. Crystal and refinement data for the ambient and highest pressure studies of **1**F and **1**MeO are given in Table 1.

	1F		**1**MeO	
Pressure (GPa)	Ambient	5.4	Ambient	5.5
Chemical formula	$C_{14}H_{10}F_2N_2NiO_4$	$C_{14}H_{10}F_2N_2NiO_4$	$C_{16}H_{16}N_2NiO_6$	$C_{16}H_{16}N_2NiO_6$
M_r	366.95	366.95	391.02	391.02
Crystal system, space group	Tetragonal, $P4_2/mbc$	Tetragonal, $P4_2/mbc$	Monoclinic, $P2_1/n$	Monoclinic, $P2_1/n$
a, *b*, c (Å)	14.5536 (10), 14.5536 (10), 6.3883 (8)	13.8998 (17), 13.8998 (17), 5.644 (4)	8.3859 (5), 4.9006 (3), 18.8884 (12)	7.8802 (8), 4.5129 (4), 17.5383 (16)
β (°)	90	90	95.598 (5)	95.233 (8)
V (Å^3)	1353.1 (2)	1090.5 (8)	772.53 (8)	621.11 (10)
Z	4	4	2	2
Radiation type	Mo *K*a, λ = 0.71073 Å	Synchrotron, λ = 0.68890 Å	Mo *K*α, λ = 0.71073 Å	Synchrotron, λ = 0.51590 Å
μ (mm^{-1})	1.48	0.24	1.29	1.61
Crystal size (mm)	0.28 × 0.12 × 0.07	0.18 × 0.16 × 0.10	0.39 × 0.05 × 0.05	0.19 × 0.16 × 0.15
T_{min}, T_{max}	0.08, 0.90	0.69, 0.98	0.79, 0.94	0.65, 0.78
No. of measured, independent and observed [$I > 2.0\sigma(I)$] reflections	4940, 660, 500	3919, 283, 216	7448, 1362, 1128	3838, 609, 519
R_{int}	0.062	0.075	0.038	0.041
$R_1[F > 4\sigma(F)]$, $wR_2(F^2)$, S	0.034, 0.096, 0.98	0.040, 0.116, 1.11	0.030, 0.032, 1.11	0.031, 0.077, 1.03
No. of reflections	660	281	1362	571
No. of parameters	77	82	136	140
No. of restraints	10	117	38	80
$\Delta\rho_{max}$, $\Delta\rho_{max}$ (e Å^{-3})	0.44, -0.48	0.70, -0.54	0.42, -0.39	0.34, -0.36
Completeness (%)	100	64	100	43.7

Table 1. Crystallographic Data for **1**F and **1**MeO. The temperature was 298 K in all cases.

2.4 Electronic structure calculations

Periodic electronic structure calculations were carried out using plane-wave density functional theory (CASTEP).[34] The PBE exchange-correlation functional[35] was used with pseudopotentials generated by the program. Basis set cut-off energies were 410 and 420 eV for the fluoro and methoxy complexes, respectively. Brillouin zone integrations were performed on a symmetrized Monkhorst-Pack *k*-point grid with spacing 0.1 $Å^{-1}$.[36] Both the k-point spacing and the basis set cut-off are chosen to ensure total energies converged to better than 0.1 meV per atom. The ambient pressure X-ray crystal structures were used as starting points for each calculation; the unit cell dimensions were held fixed while atomic coordinates were optimised, taking space group symmetry into account. The total energy convergence tolerance was $2x10^{-5}$ eV per atom, with a maximum force tolerance of 0.05 eV $Å^{-3}$, a maximum displacement of 0.002 Å and a maximum stress tolerance of 0.01 GPa. The root-mean-square fits of the non-H atom positions within clusters of 15 molecules in the observed and optimised crystal structures were < 0.001 Å and 0.024 Å at ambient pressure and 5.4 GPa, respectively.[37]

Single molecule electronic structure calculations were carried out at the B3LYP/6-311+g(d,p) level of theory (Gaussian 09)[38] using optimised geometries from the periodic DFT calculations described above. Electronic absorption spectra were calculated using the time-dependent implementation of Density Functional Theory (TD-DFT), again at the B3LYP/6-311+g(d,p) level of theory, including the first 30 excited states. For both **1**F and **1**MeO, the ground electronic state was determined to be a low-spin singlet state, consistent with the majority of square-planar nickel complexes. The high-spin triplet state was calculated to lie 0.37 eV and 0.4eV higher in energy for **1**F and **1**MeO, respectively.

2.5 Absorption spectroscopy

Visible wavelength absorption spectra were recorded using a custom-built multi-parameter microscope platform.[39] The samples were contained in the same design of diamond anvil cell as described above for the X-ray data collections, with a chip of ruby as a pressure marker A tungsten halogen light source (Ocean Optics, LS-1, fitted with a BG-34 filter) was focused, via a fused silica lens, into the sample chamber of the diamond anvil cell (DAC), mounted on a 3-axis microblock positioning stage (Thorlabs, MTB616). The transmitted light was collected by a ×15 reflecting objective (Edmund, NT58-417), forming an image around 1cm in diameter. A 500-µm diameter fused silica optical-fibre bundle (Laser 2000), connected to an Ocean Optics fibre-coupled spectrometer (USB2000+UV-VIS), was placed at the focal plane of the DAC image. The sample signal was measured by overlapping the portion of the image containing the crystal with the entrance of the optical fibre bundle, via x-y translation of the DAC. The reference (background) signal was taken from an empty part of the cell. Care was taken to avoid recording either signal within the region of the ruby chip.

2.6 High-pressure resistivity measurements

1F forms needle-like crystals, with the needle axis developed in the *c*-axis direction. We attempted to measure electrical resistivity along the *c* direction at ambient pressure using a single crystal of **1**F with four gold leads along the needle long axis. However, the resistivity was found to be higher than the measurable limit of 2×10^7 Ω cm.

In addition, several attempts were made to measure the resistivity at high pressure with the aim of testing whether the electrical conductivity of the sample is enhanced with pressure. The high-pressure resistivity measurements were carried-out in diamond anvil cell (DAC). Daphne oil was used as the pressure transmitting medium, and the pressure was determined using the ruby fluorescence technique. Measurements with single crystals were frustrated by the brittle nature of the crystals, which disintegrated even when very low pressure was applied. Data were therefore collected with a polycrystalline sample. No conductivity was detectable up to 10 GPa.

2.7 Software Used

Crystal structures were visualized using the programs MERCURY,[37] and DIAMOND.[40] Searches of the Cambridge Structural Database utilized the program CONQUEST[41] with database updates up to November 2010. The bulk moduli of the complexes were determined using the using the program EOSFIT.[42] Movies were constructed with CrystalMaker.[43]

3. Results

*3.1 The Effect of Pressure on **1**F*

Salicylaldoxime complexes were chosen for this study because these ligands self-assemble into pseudo-macrocyclic dimers through oximic OH to phenolic O hydrogen-bonds. The size of the cavity at the centre of this pseudo-macrocycle influences metal ion selectivity on complex formation.[44] We have shown that the size of this cavity is sensitive to pressure, and we are currently investigating the potential for using pressure to influence the selectivity of metal complex formation.[45]

At ambient pressure and temperature **1**F crystallises in the tetragonal space group $P4_2/mbc$. The metal occupies a site of 2/*m* (C_{2h}) symmetry which constrains the complex to be planar and centrosymmetric. The Ni has a square-planar coordination geometry with Ni-O and Ni-N distances measuring 1.832(3) and 1.874(4) Å, respectively (Table 2, Fig. 1a); the mean Ni-O/N distances in related complexes[44, 46] are 1.85(2) and 1.88(1) Å. The oximic hydrogen atom of one ligand forms bifurcated H-bonding interactions to the phenolic oxygen

[O2..O1, 2.507(4) Å] and the fluoro substituent [O2..F6, 3.618(4) Å] of the opposite ligand, generating a pseudo-macrocyclic configuration. The complexes form infinite stacks along the *c*-axis with the Ni atoms directly above and below one another; the interplanar stacking distance is 3.1942(4) Å (Fig. 1b). The molecules form layers in the *ab* plane connected by weak CH…O and CH…F contacts with H…O or F distances of between 2.42 and 2.65 Å (Fig. 1c).

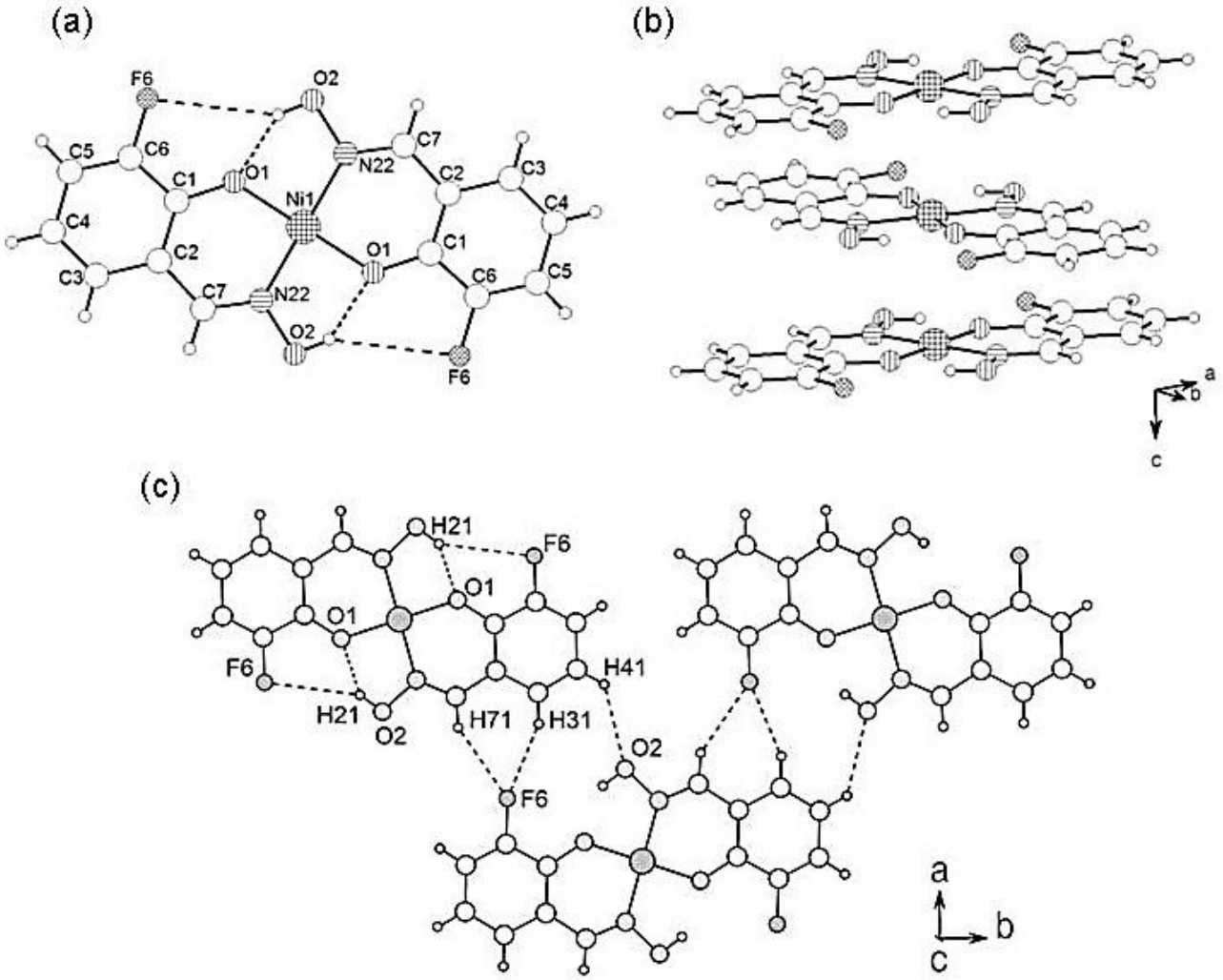

Figure 1. The crystal structure of **1**F. (a) The structure of the complex showing inter-ligand hydrogen bonding. (b) Stacks of complexes formed along the crystallographic *c*-axis direction. (c) Layers formed in the *ab* planes.

1F			**1**MeO		
Distances/Å	0 GPa	5.4 GPa	Distances/Å	0 GPa	5.6 GPa
Metal-Ligand Distances:					
Ni-N	1.874(4)	1.869(6)	Ni-N	1.872(2)	1.855(4)
Ni-O	1.832(3)	1.808(5)	Ni-O	1.824(1)	1.819(3)
Distances related to stacking:					
Ni..Ni	3.194(<0)	2.822(2)	Ni..Ni	4.9006(3)	4.5129(4)
Interplanar distance	3.194(<0)	2.822(2)	Interplanar distance	3.3401(7)	2.9363(16)
Inter-ligand H-bonding parameters:					
O(2)..O(1)	2.507(4)	2.479(8)	O(2)...O(1)	2.497(2)	2.458(6)
O(2)-H(21) ...O(1)	1.710(4)	1.761(19)	O(2)-H(21) ...O(1)	1.780(14)	1.75(2)
H-bonding parameters for 'butressing' H-bonds:					
F(6)...O(2)	3.618(4)	3.535(7)	O(2)…O(6)	3.504(2)	3.467(6)
O(2)-H(21) ...F(6)	2.892(4)	2.796(19)	O(2)-H(21) ...O(6)	2.743(5)	2.747(2)

Table 2. Distances (Å) in **1**F and **1**MeO at ambient and high pressures.

1F exhibits reversible piezochromism. As pressure increases the crystal gradually changes colour from green at ambient pressure to red at 6.1 GPa (Fig. 2); removal of pressure re-establishes the green colour of the crystal. As pressure is increased, the crystal structure remains in a compressed form of the phase formed under ambient conditions. The unit cell dimensions compress anisotropically, the *a/b* and *c*- axes shortening by 4.6% and 14.4%, respectively (Fig. 3a). The bulk modulus (K_0) and its pressure-derivative (K'), derived from a fit of the unit cell volume versus pressure data to a third-order Birch–Murnaghan equation of state[47] (Fig. 3b), are 9.1(17) GPa and 10(3).

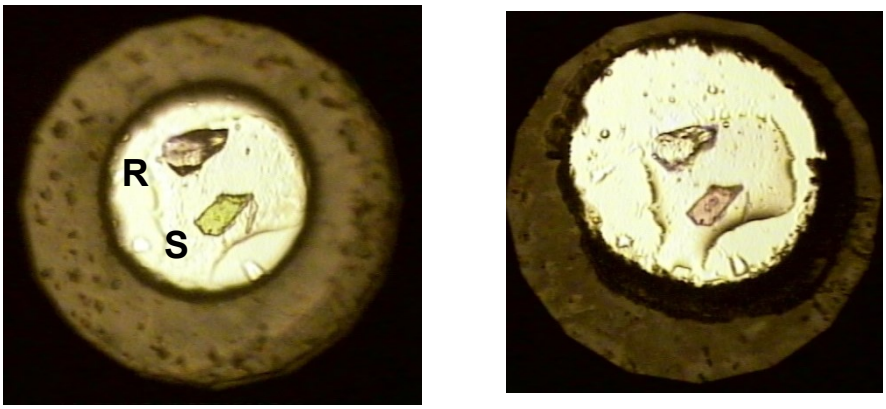

Figure 2. Piezochromism in **1**F. The figures show a sample of **1**F contained in a diamond anvil cell at near ambient pressure (a) and at 6.6 GPa (b). In (a) the labels 'R' and 'S' indicate the ruby pressure marker and the crystal of **1**F, respectively.

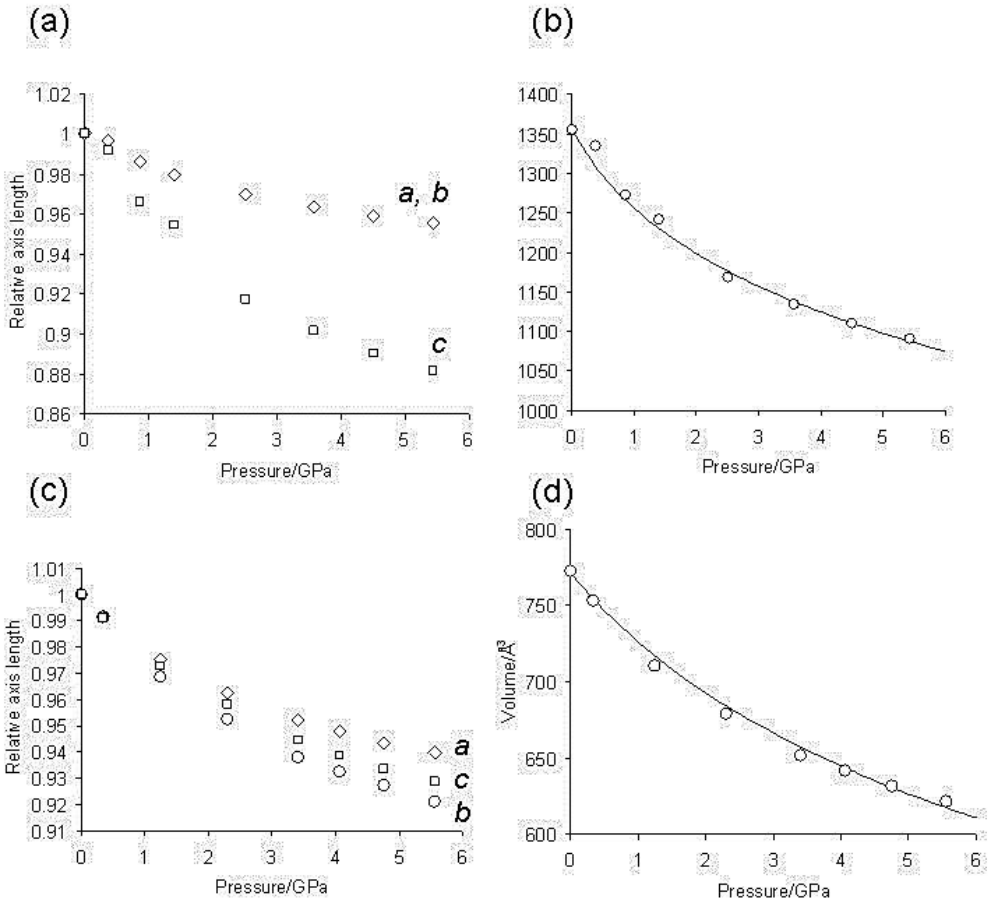

Figure 3. (a) Changes in the cell dimensions of **1**F with pressure. (b) Effect of pressure on the unit cell volume of **1**F. The trend line corresponds to a third-order Birch-Murnaghan equation of state. (c) and (d) show the equivalent data for **1**MeO.

The variation in the Ni1-O1 and Ni1-N22 distances with pressure are shown in Fig. 4a. The variation of both distances with pressure is linear within the error bars. The fitted lines have gradients equal to -0.0038 and -0.0019 Å GPa^{-1} for Ni1-O1 and Ni1-N22, respectively, indicating that the Ni-O bond is more compressible. Overall, the average reduction in the distances up to 5.4 GPa is *ca.* 0.015 Å as judged from the straight line fits. This is a substantially smaller reduction than is seen for the oxygen atom to centroid in high-pressure crystal structures of the free salicylaldoximes,[45] which form the same pseudomacrocyclic configuration as seen in the metal complexes. The size of the cavity at the centre of the macrocycle in the uncomplexed ligands can be defined as half the mean N…N and O…O distance; for 3-chlorosalicylaldoxime this parameter changes from 1.984(1) Å at ambient pressure to 1.92(1) Å at 5 GPa, a reduction of 0.06 Å. At 5.4 GPa the intramolecular H-bonding interactions in **1**F measure 2.479(8) (O2…O1) and 3.535(7) Å (O2…F6), corresponding to contractions of 0.028(9) and 0.083(8) Å, respectively.

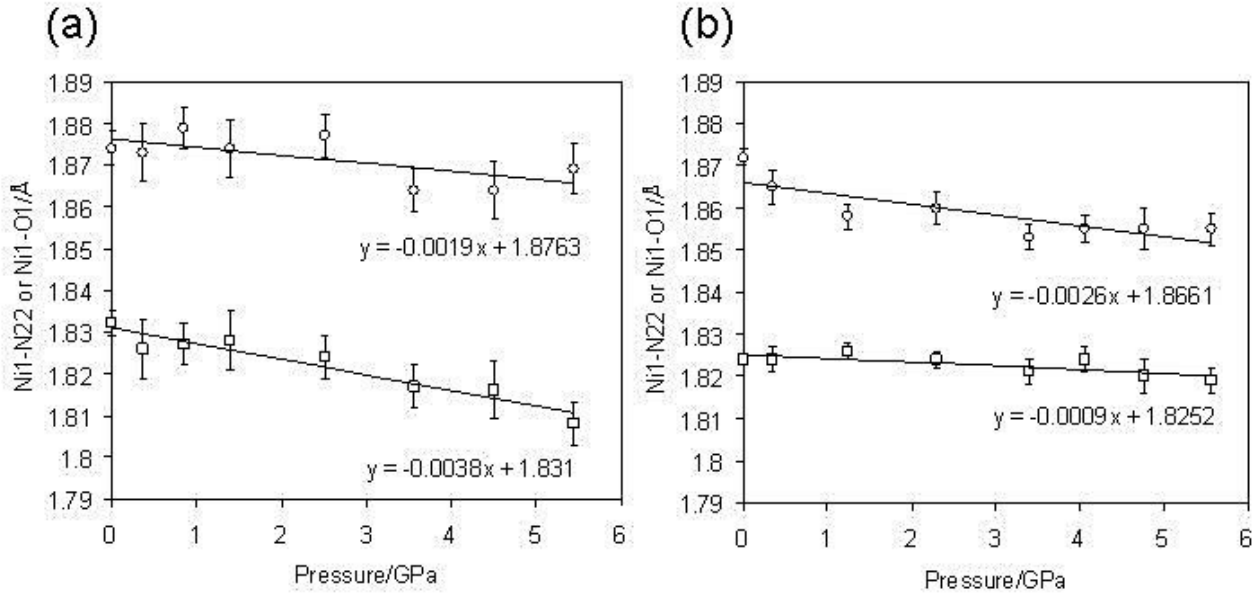

Figure 4. Variation with pressure of the Ni-N and Ni-O bond distances in (a) **1**F and (b) **1**MeO.

The changes in intermolecular distances are substantially greater than those which occur within the complexes. The interplanar stacking distance reduces by 0.372(2) Å to 2.822(2) Å, becoming comparable to Ni…Ni distances in semiconductors such as $[MePh_3P][Ni(dmit)_2]_3$ [2.7837(7) Å, CSD REFCODE REHFIT][48] and $[Ni(diiminobenzosemiquinonato)_2]_3Cl_2$ [2.804 Å, TAYYOI].[49] In spite of this geometrical similarity, high-pressure resistivity measurements showed that the sample remains insulating up to 10 GPa, with no on-set of semiconducting properties.

The effect that this has on the structure is conveniently visualised in the form of a Quicktime® movie available in the supplementary material (*Movie_1_1F_along_a.mov*). In plane H…O and H…F distances span the range 2.19 Å (F6...H71) to 2.34 Å (O2...H41). A movie (*Movie_2_1F_along_c.mov*) composed of space-filling plots of the layers formed in the *ab* plane shows that the 'bumps' on the surface of one molecule move into the 'grooves' on the surface of its neighbours. The path of compression is thus determined by the filling of interstitial void space.

*3.2 The Effect of Pressure on **1**MeO*

1MeO crystallises in space group $P2_1/n$ with the nickel atom on a centre of inversion. The molecule is essentially planar, with the largest deviation from the mean plane being 0.095(3) Å for C61 (Fig. 5a). The distances from the nickel to the N and O donor atoms are 1.8721(15) and 1.8241(14) Å, respectively, the latter being slightly shorter than in **1**F. A bifurcated pair of H-bonding interactions similar to those seen in **1**F is

formed between O2…O1 [2.497(2) Å] and O2..O6 [3.504(2) Å].

The molecules form infinite stacks along the *b* direction of the unit cell (Fig. 5b). The stacking distance, 3.34 Å, is a little longer than in the fluoro complex, but in contrast to **1**F the molecules are off-set perpendicular to the stacking direction with a slippage distance equal to 2.08 Å. The offset means that a methyl group of one molecule is located directly below the hydroxyl and methoxy groups of another molecule, and it is possible that this accounts for the longer stacking distance in the methoxy complex. The Ni…Ni distance within the stacks is 4.9006(3) Å. In **1**F the planes of the molecules are perpendicular to the stacking direction; in **1**MeO the molecules are inclined at an angle of 47°. The consequence of this is that molecules in neighbouring stacks interact along the *c*-direction in a herring-bone motif in which the angle between the molecular planes is 86°, the interaction being mediated by CH…π contacts between phenyl groups in which C5H51…C4 measures 2.81 Å (Fig.5c). Along the *a*-direction stacks are connected by C7H71…O2 contacts [C…O = 3.315(2) Å] (Fig. 5d).

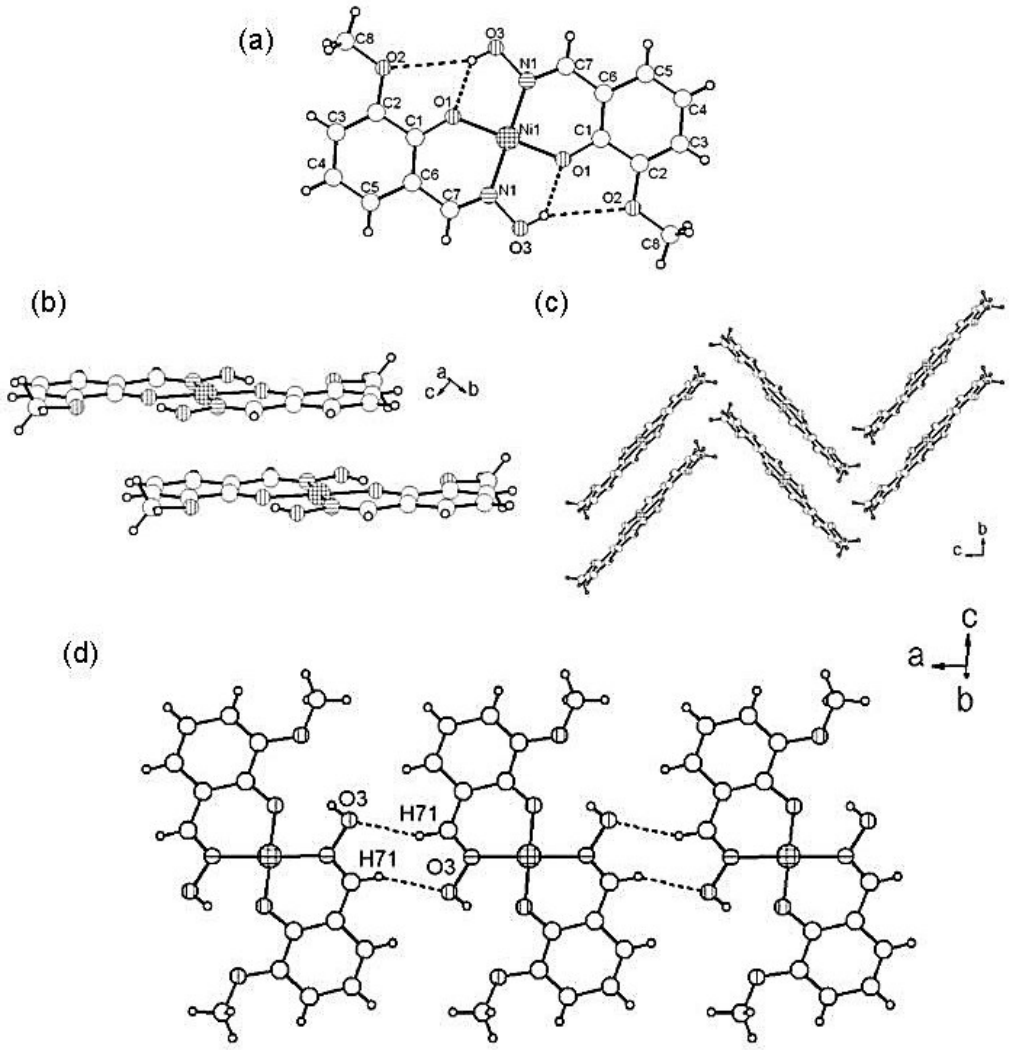

Figure 5. The crystal structure of **1**MeO. (a) The structure of the complex showing inter-ligand hydrogen

bonding. (b) Stacks of complexes formed along the crystallographic *b*-axis direction. (c) and (d) Interactions between stacks.

Like **1**F, **1**MeO is piezochromic, becoming red at 5 GPa. This change is not accompanied by a phase transition, and the crystal remains in a compressed form of its ambient pressure structure. The variation of Ni-O and Ni-N distances with pressure is shown in Fig. 4b. The rate of compression in the Ni1-O1 bond is rather less than Ni1-N22 (-0.0009 *versus* -0.0026 Å GPa^{-1}). The intramolecular O2H21…O1 H-bonding interaction shortens by 0.039(6) Å to 2.458(6) Å. Corresponding data for the 'buttressing' O2H21…O6 contact are 0.037(6) and 3.467(6) Å.

The bulk modulus and its pressure derivative [K_0 = 9.7(10) GPa and K' = 9.8(16)] are not significantly different from those reported above for the fluoro complex. Compression is quite isotropic, with the *a*, *b*, and *c* unit cell axes decreasing in length by 6, 8 and 7% respectively (Fig. 3c,d). As was the case in **1**F, the stacking direction is most sensitive to pressure. The stacking distance at 5.6 GPa is 2.94 Å, a reduction of 0.40 Å, similar to the 0.37 Å seen in **1**F. The CH…π interaction connecting stacks in the *c* direction compresses by 0.38 Å to 2.47 Å. The effect that these changes have on the herringbone packing motif can be visualised in a movie (*Movie_3_1MeO_along_a.mov*) of the series viewed along the *a* axis, which is available in the supplementary material. In the *a* direction the molecules approach one another edge-to-edge, filling interstitial voids in a similar fashion to that observed in the *ab* plane of **1**F. Here the molecules are not constrained to be coplanar and they can inter-leave to some extent (see movie *Movie_4_1MeO_along_bc.mov*). The inter-stack C7H71…O3 contacts are compressed by a similar amount to the other principal contacts, reaching 2.956(7) Å at 5.6 GPa.

3.3 Electronic absorption spectra

The electronic absorption spectra of **1**F recorded in THF solution and in the crystalline state at ambient pressure and 6.1 GPa are shown in Fig. 6a. The wavelength range over which the crystal absorption spectra can be measured is limited to 350-800 nm by the spectral output of the lamp used in the measurements, and the onset of strong absorption by the diamonds at wavelengths below 400 nm.

The solution phase spectrum of **1**F consists of a strong absorption in the UV region, with a distinct shoulder at 450 nm (ε = 177.5 $M^{-1}cm^{-1}$) and significantly weaker band in the visible at 620 nm (ε = 67 $M^{-1}cm^{-1}$). The pale green colour of the solution corresponds to the optical window, at around 535 nm, created by the tails of the shoulder at 450 nm and the band at 620 nm. The positions of the absorption maxima in the crystalline sample at ambient pressure are similar those in the solution phase spectrum, with bands observed at 625 nm and 450 nm. Similar comments can be made with regard to the absorption spectra of **1**MeO (Fig. 6b), which show

corresponding absorptions at 620 and 440 nm in the crystalline state at ambient pressure.

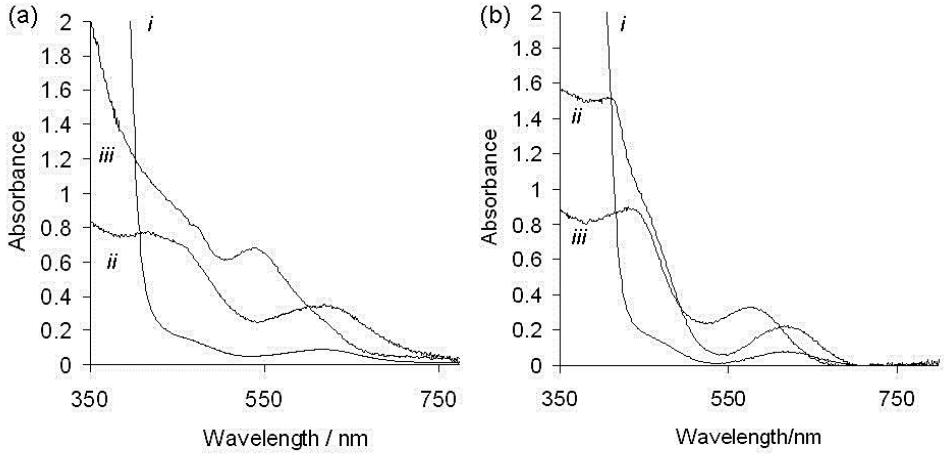

Figure 6. UV-visible spectra of (a) **1**F and (b) **1**MeO in solution (i) and in the crystalline state at ambient pressure (ii) and ~6 GPa (iii).

Application of pressure results in a marked blue shift in the longer wavelength absorption bands, from 620 to 540 nm at 6.1 GPa in **1**F and from 620 to 580 nm at 5.5 GPa in **1**MeO. The shorter wavelength bands are also blue-shifted: the 440-nm band of **1**MeO to 410 nm while the 450-nm band of **1**F becomes hidden under the shoulder of an intense higher energy absorption .

4. Discussion

4.1 Comparison of the effects of pressure on 1F and 1MeO

The crystal structures of both **1**F and **1**MeO consist of stacks of molecules. In **1**MeO the stacking is off-set, whilst in **1**F the Ni atoms lie above and below each other. The bulk moduli, which measure the resistance of the crystal to compression, are similar with $K \sim 9$ GPa and $K' \sim 10$, reflecting the underlying similarity of the intermolecular interactions. The materials are softer than a typical hydrogen-bonded system such as the amino acid L-alanine [$K_0 = 13.1$ GPa, $K' = 7.1(3)$],[50] but quite similar to bis(dimethylglyoximato)nickel(II) [$K_0 = 8.0(4)$ GPa, $K' = 11.0(7)$].[51]

Compression of **1**F is markedly more anisotropic than **1**MeO. This reflects the different intermolecular interactions which are formed along different crystallographic directions in **1**F: the molecules stack along the *c* direction, while they interact in an edge-wise fashion in the *a* and *b* directions. The stacking interaction is

the softer of the two. In the *ab* planes the molecules fill void space, avoiding overlap of van der Waals envelopes. In **1**MeO the orientations of the two molecules within each unit cell are different, and the intermolecular interactions are distributed in different crystallographic directions, making the overall compression of the unit cell more isotropic than in **1**F. **1**MeO crystallises in a non-orthogonal crystal system, and it is more informative to examine the effect of pressure using the strain tensor rather than simply examining changes in the unit cell lengths.[1] The smallest eigenvalue of the strain tensor, corresponding to the least compressible direction, is approximately aligned with the *a*-axis (the angle between the two directions is 16°), which also corresponds to compression of molecules in an edge-wise fashion.

While intermolecular interactions are subject to the largest changes, metal-ligand bond distances are also effected by pressure. Symmetry constrains molecules to be pushed edge-to-edge directly against each other in **1**F, whereas in **1**MeO the molecules can interleave. The average compression of the Ni-ligand bonds is therefore greater in **1**F. In **1**F the Ni-O bond is more compressible than the Ni-N bond. In **1**MeO the Ni-O bond distance hardly varies with pressure at all, while the Ni-N bond compresses by a similar amount to that observed in **1**F. This difference correlates with the distribution of voids in the regions corresponding to compression of the edge-to-edge contacts. In **1**F the Ni-N bonds are oriented towards larger voids than the Ni-O bonds, and the Ni-O bonds are therefore more strongly affected by compression. The path of compression can be visualised in the movie *Movie_1_1F_along_c.mov* available in the supplementary material. The situation is reversed in **1**MeO: here it is the Ni-N bonds which are directed towards small voids formed in the region in which edge-to-edge contacts are compressed, whereas the Ni-O bonds point towards a void that is still present even at 5.6 GPa (see *Movie_5_1MeO_edge_to_edge.mov*).

Compression of the geometry of the metal ions is much less than compression of the cavity formed at the centre of the pseudomacrocycles in the structures of the free ligands, the difference reflecting the buttressing effect of a metal ion *versus* inter-ligand H-bonds. Nevertheless, the significance of packing effects in determining the response of intramolecular geometry to pressure is reminiscent of effects noted for the complex $[Mn_{12}O_{12}(O_2CCH_2{}^tBu)_{16}(H_2O)_4]\cdot CH_2Cl_2\cdot MeNO_2$ (see *Introduction*) where the direction of a Jahn-Teller axis can be reorientated, causing a dramatic change in magnetic properties as the result of local strain generated as molecules are pushed together.[13]

*4.2 Comparison of the effects of pressure on **1**F and **1**MeO with those in nickel glyoximate complexes*

The systems most closely related to **1**F and **1**MeO that have been studied previously at high pressure are the Ni, Pd and Pt complexes of glyoximato ligands.[24, 52] The first of these complexes to be crystallographically

[1] The strain tensor is an ellipsoid which expresses the overall effect of pressure on a crystal structure, revealing the directions which undergo the greatest and least compression. The lengths and directions of the axes of the ellipsoid are the eigenvalues and eigenvectors of the strain tensor, and in a monoclinic crystal one of these must lie along the *b* axis by symmetry.

characterised at ambient pressure was $Ni(dmg)_2$ (dmg = dimethylglyoximato).[53] The crystal structure contains planar complexes arranged in infinite stacks with neighbouring molecules rotated by 90° with respect to each other. The Ni atoms lie directly above and below one another, with a Ni…Ni distance of 3.183 Å in the most recent determination at 130 K (NIMGLO12),[54] a value which has been interpreted as implying metal-metal bonding. These features resemble those described here for **1**F.

Though the stacked motif with short Ni…Ni bonds is common, there are exceptions in which the molecules are displaced or rotated in a direction perpendicular to the stacking direction, as seen in the crystal structure of **1**MeO. This effect increases the Ni…Ni distance to 3.8 Å and above, and can be exemplified by the Ni complex of glyoxime itself, in which the Ni…Ni distance is 4.210 Å [NIGLOX01 and 10].[55]

One derivative, $[Ni(emg)_2]$ (emg = ethyl-methyl-glyoximato), exhibits polymorphism, the α-form crystallising with a slipped stacking interaction and a Ni…Ni distance of 4.750 Å [NIMEGL01],[56] while the rarer β form crystallises with parallel stacks and a Ni…Ni distance of *ca* 3.4 Å.[57]

The effect of pressure on the crystal structure of $[Ni(dmg)_2]$ has been studied up to 7.4 GPa using X-ray powder diffraction;[51] the similarity of the bulk moduli of this material with those of **1**F was referred to above. Full sets of atomic coordinates were not obtained in this study, though the Ni…Ni distance, inferred from the length of the *c*-axis, decreases by a very similar amount to that seen in **1**F (3.26 Å at ambient temperature and pressure to 2.82 Å at 7.4 GPa). However, by contrast to **1**F, this shortening is accompanied by a substantial decrease in resistivity with pressure, reaching 50 Ω cm at 23 GPa.[51]

Much of the interest in nickel glyoximato complexes, both at ambient and at high pressure, was derived from their spectroscopic properties. Solid-state UV-visible spectra of derivatives which have short Ni…Ni interactions exhibit a strong, sharp band at *ca*. 500 nm.[58] This band is absent in solution spectra, implying that its origin lies in the close intermolecular contacts. In support of this, in the α-form of $Ni(emg)_2$ the band is present, but very weak, while it the β form it is strong.[58b] The band has been assigned to a $3d(z^2) \rightarrow 4p(z)$ transition.[58c] In the free molecules this transition occurs at high energy beyond the visible region, but in the crystal the presence of positive metal ions on the *z*-axis, directly above and below the molecule, decreases the energy of the 4p(*z*) orbital, bringing the transition into the visible region.[24] The high intensity of the band is due to 'intensity borrowing' from a high energy band around 200 nm, which has been assigned to a charge transfer transition from the $3d(z^2)$ orbital on one Ni to the 4p(*z*) orbital on a neighbouring Ni.[58c] This band is observed in the β form of $Ni(emg)_2$, but not in the α form, and this is thought to be why the 500 nm band is present but weak in the latter.

Drickamer measured UV-visible spectra of a number of Ni, Pd and Pt glyoximate complexes as a function of pressure.[52] In all cases the initial effect of pressure was to cause the absorption band to move to substantially lower energy, by 6100 cm^{-1} for $Ni(dmg)_2$ at 10 GPa. This supports the electrostatic explanation for the lowering of the energy of this transition in moving from the solution to the solid state. Application of pressure

also caused the intensity of the band to decrease. In the case of one complex, bis(cycloheptoximato)platinum(II),[52a] the change in intensity precisely mirrored the blue shift of the high energy band with pressure, as inferred from its tail in the visible region. Since this effect causes the energy difference between the two transitions to increase, intensity borrowing is reduced, and the 500 nm band becomes weaker with pressure. This work provides a nice example of the way in which high pressure can be used to help verify structure- spectroscopic property relationships.

*4.3 The origin of piezochromism in **1**F and **1**MeO*

Although the crystal structure of **1**F consists of closely spaced stacks of molecules, its UV-visible spectrum lacks the strong, sharp band at *ca* 500 nm characteristic of glyoximate complexes. The spectrum of **1**F is essentially the same in the solid and solution states, while **1**F and **1**MeO have very similar spectra (Fig. 6), in spite of their quite different crystal structures. The implication is that, by contrast to the glyoximato complexes, crystal packing effects have only a modest influence on the UV-visible spectra of salicylaldoximate complexes.

Pressure has a different effect on the position of the absorption bands in spectra of glyoximate and salicylaldoximate complexes, with the red shift in the former being replaced by a blue shift in the latter. Both **1**F and **1**MeO gradually change from being green at ambient pressure to red at 5 GPa. This colour change is associated with the shift of the band at 620 nm to 540 nm in **1**F and to 580 nm in **1**MeO which decreases transmission of green light and increases transmission of red light with wavelengths above 650 nm.

The similarity of the responses to pressure seen in the spectra of **1**F and **1**MeO, together with the apparent lack of intermolecular effects demonstrated in the ambient pressure solution and solid state spectra, suggest that the origin of the piezochromism described here is intramolecular, not intermolecular as in glyoximate complexes. This implies that there is a difference in the band structures of these two families of nickel complex which exists in spite of the similarities in their crystal structures. This is also reflected in their different electrical properties at high pressure, the glyoximate complexes becoming conductors, the salicylaldoximate complexes retaining their insulating properties.

The low extinction coefficient measured for the 620 nm band in **1**F and **1**MeO is consistent with its originating from a Laporte-forbidden d-d transition. Time-dependent DFT calculations on **1**F indicate that d-d transitions could be observed at 731, 612, 534 and 462 nm. All are Laporte forbidden, and those at 612 and 462 nm, corresponding to transitions involving d(z^2) → d(x^2-y^2) and d(xy) → d(x^2-y^2), are in reasonable agreement with the observed bands at 620 and 450 nm. The pressure-induced shift in the first of these is reproduced well by the calculations, obs: 60 nm, from 620 to 540 nm, calc: 72 nm, from 612 to 540 nm.

The destination orbital for the 620 nm transition involves a σ* interaction based on Ni d(x^2-y^2). The calculations show that the energy of this orbital is more sensitive than any other to the Ni-N and Ni-O bond distances. Since this orbital is anti-bonding, it becomes destabilised as the interactions shorten (Fig 7), so that transitions into this orbital occur at higher energy. This leads to the conclusion that the piezochromism on **1**F and **1**MeO is the result of the pressure-tuning of the crystal field about the Ni atom through control of the Ni-O and N bond distances.

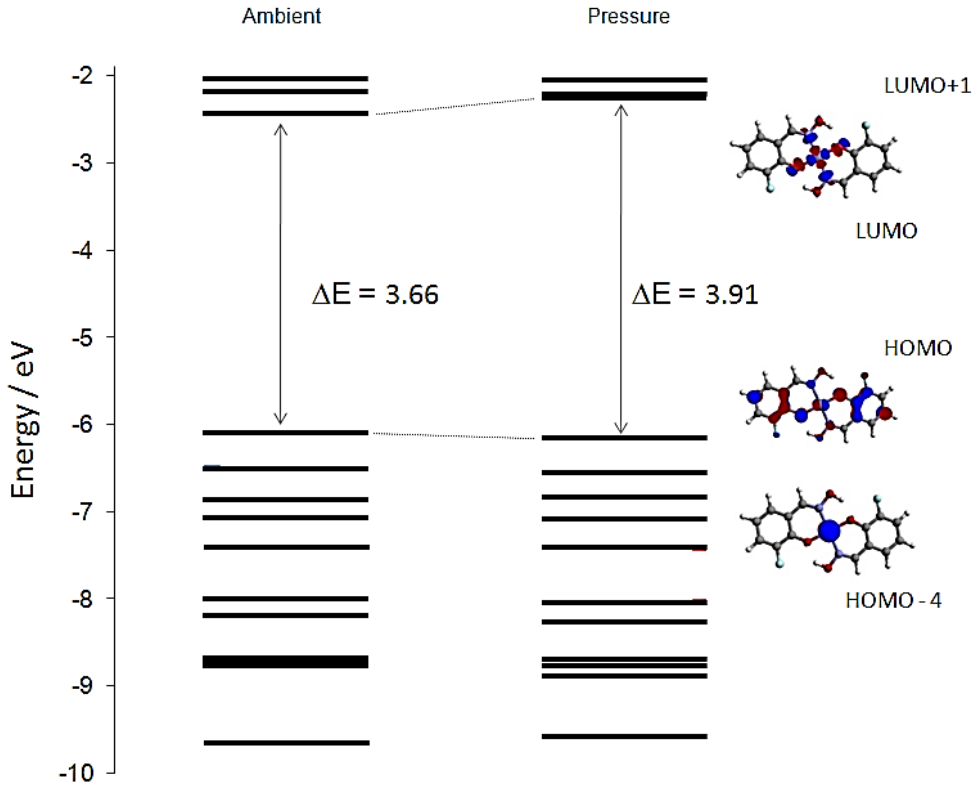

Figure 7. Energy of the calculated frontier molecular orbitals for **1**F calculated for the geometries observed at ambient pressure (left) and 6 GPa (right). Energies are in eV.

Although the piezochromism of **1**F and **1**MeO is primarily intramolecular in origin, intermolecular interactions do have an influence because they control the amount by which the Ni-O and Ni-N distances are shortened with pressure. It was shown above that the extent of shortening correlated with whether or not the bond in question was oriented towards an interstitial void. When estimated from the straight line fits in Fig. 4, the average the shortening of bonds in **1**MeO at 6 GPa is about 60% of that experienced by the bonds in **1**F at the same pressure. This difference correlates with the smaller blue shift observed in the UV-visible spectra of **1**MeO (40 versus 80 nm in **1**F).

5. Conclusions

It was initially assumed that the effects of pressure on the crystal structures and UV-visible spectra of the nickel salicylaldoximate complexes **1**F and **1**MeO might arise from changes in intermolecular contacts. Both complexes adopt the expected square-planar geometry characteristic of other Ni salicylaldoximate complexes,[44] and in **1**F the molecules pack in stacks with short Ni…Ni distances of around 3.2 Å, whilst in **1**MeO stacks are off-set to give longer Ni…Ni distances. Whilst the most prominent effect of pressure (up to *ca* 6 GPa) is to compress intermolecular distances, the intramolecular Ni-N and O distances are also compressed by an average of 0.017 Å in **1**F and 0.011 Å in **1**MeO. The smaller value for **1**MeO correlates with the orientation of the Ni-O and Ni-N bonds towards interstitial voids, so that edge-to-edge compression is less than in **1**F.

The origin of the piezochromism in **1**F and **1**MeO which change colour from green at ambient pressure to red at above 5 GPa, is different from that which has been observed in group 10 glyoximate complexes for which high-pressure UV-visible spectra indicate that the red shift occurs in a strong nd→(n+1)p transition associated with the presence of short metal-metal contacts. Although such contacts are also present in **1**F, there is no trace of a similar band in its UV-visible spectrum, which is very similar to those obtained for the same compound in solution and for **1**MeO. By contrast to the glyoximate complexes, the strongest bands in the UV-visible spectra of **1**F and **1**MeO originate from d-d transitions, and these become blue shifted with pressure. It is this blue shift that is responsible for the piezochromism, and it can be traced to the destabilisation of a d(x^2-y^2) orbital which occurs as the Ni-O and N bonds shorten with pressure and 'tune' the crystal field experienced by the metal atom.

7. References

[1] V. H. Crawford, H. W. Richardson, J. R. Wasson, D. J. Hodgson and W. E. Hatfield, *Inorganic Chemistry* **1976**, *15*, 2107-2110.

[2] a) E. V. Boldyreva, *Acta Crystallographica, Section A: Foundations of Crystallography* **2008**, *A64*, 218-231; b) E. V. Boldyreva, H. Ahsbahs, V. V. Chernyshev, S. N. Ivashevskaya and A. R. Oganov, *Zeitschrift fuer Kristallographie* **2006**, *221*, 186-197; c) S. A. Moggach, S. Parsons and P. A. Wood, *Crystallography Reviews* **2008**, In press.

[3] R. D. L. Johnstone, D. Francis, A. R. Lennie, W. G. Marshall, S. A. Moggach, S. Parsons, E. Pidcock and J. E. Warren, *CrystEngComm* **2008**, ***10(12)***, 1758-1769.

[4] D. R. Allan, A. J. Blake, D. Huang, T. J. Prior and M. Schroeder, *Chemical Communications* **2006**, 4081-4083.

[5] F. H. Allen and W. D. S. Motherwell, *Acta Crystallographica, Section B* **2002**, *58*, 407-422.

[6] C. Slebodnick, J. Zhao, R. Angel, B. E. Hanson, Y. Song, Z. Liu and R. J. Hemley, *Inorganic Chemistry* **2004**, *43*, 5245-5252.

[7] N. Casati, P. Macchi and A. Sironi, *Angew. Chem., Int. Ed. Engl.* **2005**, *44*, 7736-7739.

[8] G. M. Espallargas, L. Brammer, D. R. Allan, C. R. Pulham, N. Robertson and J. E. Warren, *Journal of the American Chemical Society* **2008**, ***130(28)***, 9058-9071.

[9] N. Casati, P. Macchi and A. Sironi, *Chem.--Eur. J.* **2009**, *15*, 4446-4457.

[10] S. A. Moggach, K. W. Galloway, A. R. Lennie, P. Parois, N. Rowantree, E. K. Brechin, J. E. Warren, M. Murrie and S. Parsons, *CrystEngComm* **2009**, *11*, 2601-2604.

[11] S. Tancharakorn, F. P. A. Fabbiani, D. R. Allan, K. V. Kamenev and N. Robertson, *J. Am. Chem. Soc.* **2006**, *128*, 9205-9210.

[12] A. Prescimone, C. J. Milios, S. A. Moggach, J. E. Warren, A. R. Lennie, J. Sanchez-Benitez, K. Kamenev, R. Bircher, M. Murrie, S. Parsons and E. K. Brechin, *Angew Chem Int Ed Engl* **2008**, *47*, 2828-2831.

[13] P. Parois, S. A. Moggach, J. Sanchez-Benitez, K. V. Kamenev, A. R. Lennie, J. E. Warren, E. K. Brechin, S. Parsons and M. Murrie, *Chem. Comm.* **2010**, DOI: 10.1039/B923962F.

[14] T. Granier, B. Gallois, J. Gaultier, J. A. Real and J. Zarembowitch, *Inorg. Chem.* **1993**, *32*, 5305-5312.

[15] V. Legrand, F. Le Gac, P. Guionneau and J. F. Letard, *Journal of Applied Crystallography* **2008**, *41*, 637-640.

[16] a) S. A. Moggach, T. D. Bennett and A. K. Cheetham, *Angewandte Chemie* **2009**, In press; b) T. D. Bennett, P. Simoncic, S. A. Moggach, F. Gozzo, P. Macchi, D. A. Keen, J.-C. Tan and A. K. Cheetham, *Chem. Commun. (Cambridge, U. K.)* **2011**, *47*, 7983-7985; c) D. Fairen-Jimenez, S. A. Moggach, M. T. Wharmby, P. A. Wright,

S. Parsons and T. Duren, *Journal of the American Chemical Society* **2011**, *133*, 8900-8902; d) A. J. Graham, D. R. Allan, A. Muszkiewicz, C. A. Morrison and S. A. Moggach, *Angew. Chem., Int. Ed.* **2011**, No pp yet given.

[17] a) C. Reber, J. K. Grey, E. Lanthier and K. A. Frantzen in *Pressure-induced change of d-d luminescence energies, vibronic structure, and band intensities in transition metal complexes*, *Vol.* Eds.: J. P. Fackler and L. R. Falvello), **2011**, pp. 181-199; b) J. K. Grey and I. S. Butler, *Coord. Chem. Rev.* **2001**, *219-221*, 713-759.

[18] R. W. Parsons and H. G. Drickamer, *J. Chem. Phys.* **1958**, *29*, 930-937.

[19] F. Rodriguez, F. Aguado, R. Valiente, M. Hanfland and J. P. Itie, *Physica Status Solidi B: Basic Research* **2007**, *244*, 156-161.

[20] G. J. Halder, K. W. Chapman, J. A. Schlueter and J. L. Manson, *Angew. Chem., Int. Ed.* **2011**, *50*, 419-421, S419/411-S419/412.

[21] F. Aguado, F. Rodriguez, R. Valiente, J. P. Itie and P. Munsch, *Phys. Rev. B Condens. Matter Mater. Phys.* **2004**, *70*, 214104/214101-214104/214109.

[22] K. L. Bray, H. G. Drickamer, E. A. Schmitt and D. N. Hendrickson, *J. Am. Chem. Soc.* **1989**, *111*, 2849-2856.

[23] K. W. Galloway, S. A. Moggach, P. Parois, A. R. Lennie, J. E. Warren, E. K. Brechin, R. D. Peacock, R. Valiente, J. Gonzalez, F. Rodriguez, S. Parsons and M. Murrie, *Crystengcomm* **2010**, *12*, 2516-2519.

[24] H. D. Takagi, K. Noda and S. Itoh, *Platinum Met. Rev.* **2004**, *48*, 117-124.

[25] I. Shirotani, *Platinum Met. Rev.* **1987**, *31*, 20-23.

[26] a) R. Valiente, J. M. Garcia-Lastra, P. Garcia-Fernandez, S. Garcia-Revilla and O. S. Wenger, *European Journal of Inorganic Chemistry* **2007**, 5735-5742; b) O. S. Wenger, S. Garcia-Revilla, H. U. Gudel, H. B. Gray and R. Valiente, *Chemical Physics Letters* **2004**, *384*, 190-192.

[27] H. Ito, T. Saito, N. Oshima, N. Kitamura, S. Ishizaka, Y. Hinatsu, M. Wakeshima, M. Kato, K. Tsuge and M. Sawamura, *Journal of the American Chemical Society* **2008**, *130*, 10044-10045.

[28] A. Altomare, G. Cascarano, C. Giacovazzo, A. Guagliardi, M. C. Burla, G. Polidori and M. Camalli, *Journal of Applied Crystallography* **1994**, *27*, 435-435.

[29] P. W. Betteridge, J. R. Carruthers, R. I. Cooper, K. Prout and D. J. Watkin, *Journal of Applied Crystallography* **2003**, *36*, 1487.

[30] B.-W. Li, M.-H. Zeng and S. W. Ng, *Acta Crystallographica Section E* **2009**, *65*, m318.

[31] a) L. Merrill and W. A. Bassett, *Review of Scientific Instruments* **1974**, *45*, 290-294; b) S. A. Moggach, D. R. Allan, S. Parsons and J. E. Warren, *Journal of Applied Crystallography* **2008**, *41*, 249-251

[32] S. Parsons in *ECLIPSE*, *Vol.* The University of Edinburgh, Edinburgh, UK, **2004**.

[33] A. Dawson, D. R. Allan, S. Parsons and M. Ruf, *Journal of Applied Crystallography* **2004**, *37*, 410-416.

[34] S. J. Clark, M. D. Segall, C. J. Pickard, P. J. Hasnip, M. J. Probert, K. Refson and M. C. Payne, *Z. Krist.* **2005**, *220*, 567-570.

[35] J. P. Perdew, K. Burke and M. Ernzerhof, *Physical Review Letters* **1996**, *77*, 3865.

[36] H. J. Monkhorst and J. D. Pack, *Physical Review B* **1976**, *13*, 5188-5192.

[37] C. F. Macrae, I. J. Bruno, J. A. Chisholm, P. R. Edgington, P. McCabe, E. Pidcock, L. Rodriguez-Monge, R. Taylor, J. van de Streek and P. A. Wood, *Journal of Applied Crystallography* **2008**, *41*, 466-470

[38] M. J. Frisch, G. W. Trucks, H. B. Schlegel, G. E. Scuseria, M. A. Robb, J. R. Cheeseman, G. Scalmani, V. Barone, B. Mennucci, G. A. Petersson, H. Nakatsuji, M. Caricato, X. Li, H. P. Hratchian, A. F. Izmaylov, J. Bloino, G. Zheng, J. L. Sonnenberg, M. Hada, M. Ehara, K. Toyota, R. Fukuda, J. Hasegawa, M. Ishida, T. Nakajima, Y. Honda, O. Kitao, H. Nakai, T. Vreven, J. J. A. Montgomery, J. E. Peralta, F. Ogliaro, M. Bearpark, J. J. Heyd, E. Brothers, K. N. Kudin, V. N. Staroverov, R. Kobayashi, J. Normand, K. Raghavachari, A. Rendell, J. C. Burant, S. S. Iyengar, J. Tomasi, M. Cossi, N. Rega, J. M. Millam, M. Klene, J. E. Knox, J. B. Cross, V. Bakken, C. Adamo, J. Jaramillo, R. Gomperts, R. E. Stratmann, O. Yazyev, A. J. Austin, R. Cammi, C. Pomelli, J. W. Ochterski, R. L. Martin, K. Morokuma, V. G. Zakrzewski, G. A. Voth, P. Salvador, J. J. Dannenberg, S. Dapprich, A. D. Daniels, O. Farkas, J. B. Foresman, J. V. Ortiz, J. Cioslowski and D. J. Fox in *Gaussian 09, Revision A.1*, *Vol.* Gaussian, Inc., Wallingford CT, **2009**.

[39] M. A. Bennet, P. R. Richardson, J. Arlt, A. McCarthy, G. S. Buller and A. C. Jones, *Lab Chip* **2011**, *11*, 3821-3828.

[40] K. Brandenburg and H. Putz in *DIAMOND, version 3.2, Visual crystal structure information system*, *Vol.* Crystal Impact, Bonn, Germany, **2005**.

[41] I. J. Bruno, J. C. Cole, P. R. Edgington, M. Kessler, C. F. Macrae, P. McCabe, J. Pearson and R. Taylor, *Acta Crystallographica, Section B* **2002**, *58*, 389-397.

[42] R. J. Angel in *EOSFIT version 5.2*, *Vol.* Virginia Tech, Blackburg, VA, USA, **2002**.

[43] CrystalMaker in *A crystal and molecular structures program for MAC and Windows.*, *Vol.* Oxford, UK, **2009**.

[44] A. G. Smith, P. A. Tasker and D. J. White, *Coordination Chemistry Reviews* **2003**, *241*, 61-85.

[45] a) P. A. Wood, R. S. Forgan, D. Henderson, S. Parsons, E. Pidcock, P. A. Tasker and J. E. Warren, *Acta Crystallographica, Section B: Structural Science* **2006**, *B62*, 1099-1111; b) P. A. Wood, R. S. Forgan, A. R. Lennie, S. Parsons, E. Pidcock, P. A. Tasker and J. E. Warren, *CrystEngComm* **2008**, 239 - 251; c) R. S. Forgan, P. A. Wood, J. Campbell, D. K. Henderson, F. E. McAllister, S. Parsons, E. Pidcock, R. M. Swart and P. A. Tasker, *Chemical Communications* **2007**, 4940-4942.

[46] I. J. Bruno, J. C. Cole, M. Kessler, J. Luo, W. D. S. Motherwell, L. H. Purkis, B. R. Smith, R. Taylor, R. I. Cooper, S. E. Harris and A. G. Orpen, *Journal of Chemical Information and Computer Sciences* **2004**, *44*, 2133-2144.

[47] F. Birch, *Journal of Geophysical Research, B* **1986**, *91*, 4949-4954.

[48] A. E. Pullen, H.-L. Liu, D. B. Tanner, K. A. Abboud and J. R. Reynolds, *Journal of Materials Chemistry* **1997**, *7*, 377-380.

[49] T. Kubo, M. Sakamoto, H. Kitagawa and K. Nakasuji, *Synthetic Metals* **2005**, *153*, 465-468.

[50] N. P. Funnell, A. Dawson, D. Francis, A. R. Lennie, W. G. Marshall, S. A. Moggach, J. E. Warren and S. Parsons, *CrystEngComm* **2010**, *12*, In Press.

[51] K. Takeda, J. Hayashi, I. Shirotani, H. Fukuda and K. Yakushi, *Molecular Crystals and Liquid Crystals* **2006**, *460*, 131-144.

[52] a) M. Tkacz and H. G. Drickamer, *Journal of Chemical Physics* **1986**, *85*, 1184-1189; b) J. C. Zahner and H. G. Drickamer, *Journal of Chemical Physics* **1960**, *33*, 1625-1628.

[53] L. E. Godycki and R. E. Rundle, *Acta Crystallogr.* **1953**, *6*, 487-495.

[54] A. Czapik and M. Gdaniec, *Private Communication to CCDC* **2009**, *CCDC 759570 REFCODE NIMGLO12*.

[55] a) M. Calleri, G. Ferraris and D. Viterbo, *Acta Crystallogr.* **1967**, *22*, 468-475; b) R. K. Murmann and E. O. Schlemper, *Acta Crystallogr.* **1967**, *23*, 667-669.

[56] R. H. Bowers, C. V. Banks and R. A. Jacobson, *Acta Crystallogr., Sect. B* **1972**, *28*, 2318-2322.

[57] A. G. Sharpe and D. B. Wakefield, *J. Chem. Soc.* **1957**, 281-285.

[58] a) C. V. Banks and D. W. Barnum, *Journal of the American Chemical Society* **1958**, *80*, 4767-4772; b) B. G. Anex and F. K. Krist, *Journal of the American Chemical Society* **1967**, *89*, 6114-6125; c) S. Nagakura, Y. Ohashi and I. Hanazaki, *Inorganic Chemistry* **1970**, *9*, 2551-2556.